REVIEW

Selected isotope ratio measurements of light metallic elements (Li, Mg, Ca, and Cu) by multiple collector ICP-MS

Thomas I. Platzner · Irina Segal · Ludwik Halicz

Received: 30 July 2007 / Revised: 25 September 2007 / Accepted: 1 October 2007 / Published online: 26 October 2007 © Springer-Verlag 2007

Abstract The unique capabilities of multiple collector inductively coupled mass spectrometry (MC-ICP-MS) for high precision isotope ratio measurements in light elements as Li, Mg, Ca, and Cu are reviewed in this paper. These elements have been intensively studied at the Geological Survey of Israel (GSI) and other laboratories over the past few years, and the methods used to obtain high precision isotope analyses are discussed in detail. The scientific study of isotopic fractionation of these elements is significant for achieving a better understanding of geochemical and biochemical processes in nature and the environment.

Keywords Light elements · Isotope ratio · MC-ICP-MS

Introduction

The development of multiple collector inductively coupled mass spectrometry (MC-ICP-MS) about 15 years ago immediately indicated the advantages of this technique, at least in ratio measurements from mass 80 and above. In general, the acquired data showed precision equal or better to the well-established thermal ionization mass spectrometry (TIMS) [1, 2]. The ease of data acquisition was remarkable, the ionization efficiency was significantly larger, and consequently the sensitivity was improved. When MC-ICP-MS was introduced it had to compete with TIMS, which at that time was fully developed and provided the best isotope ratio data for metallic elements in terms of precision and accuracy. Even in the stages of application tests MC-ICP-MS exhibited several advantages: high precision, high reproducibility, high analytical throughput, simple sample preparation, and, as mentioned above, improved sensitivity [3].

MC-ICP-MS requires a more complicated instrument compared to TIMS. It uses an ion source at atmospheric pressure and therefore requires a specially designed ion beam introduction inlet system equipped with efficient pumping systems to reduce the argon gas pressure to 10^{-7} – 10^{-8} mbar. Further pumping systems along the ion flight tube maintain the vacuum at 2×10^{-9} mbar. The ion beam emerging from the interface has a circular profile which requires a tunable quadrupole lens, efficiently changing it to a rectangular shape. This rectangular ion beam possesses ions with an energy spread of up to 30 eV. An electrostatic energy filter is used to separate an almost monoenergetic ion beam acceptable for the magnetic sector mass separator. A further inherent problem in an ICP-MS is the relatively high instability of the plasma, observed as fluctuations and drifts of the ion beam. A single collector system, whether a Faraday cup or an electron multiplier, is too slow to follow this instability; therefore an array of Faraday cups (and also a Daly electron multiplier) is mounted at the end of the instrument, allowing the simultaneous monitoring of two or more ion beam intensities. This technique had already been applied in the multiple collector TIMS instruments.

Plasma 54 (P54), the first MC-ICP-MS instrument manufactured by VG Elemental in the UK [1], contained an ion collector equipped with seven Faraday cups and an analog Daly detector. A unique feature of all double focusing instruments is the wide flat-topped ion peak shape, which is of primary importance for high precision data acquisition. Two further modifications were applied to this instrument: a wide-end flight tube to allow simultaneous measurement of ions with large mass differences, such as U-Pb or ⁶Li-⁷Li,

T. I. Platzner · I. Segal · L. Halicz (🖂) Geological Survey of Israel (GSI), Jerusalem 95501, Israel

e-mail: ludwik@gsi.gov.il



and the addition of an electrostatic energy filter before the Daly detector to enhance abundance sensitivity measurements. Isotope ratio measurements using laser ablation have also been demonstrated [4]. Several years later VG Elemental-Thermo Elemental introduced the Axiom, a smaller double focusing instrument of vertical configuration, providing high mass resolution capability. This mass spectrometer was aimed for high precision, fast analytical work [5].

Several other MC-ICP-MS instruments were manufactured by other companies applying different approaches for efficient reduction of ionic spectral interferences formed by argon and atmospheric gases, e.g., thermalizing the ions produced by the plasma, introducing a detection system comprising a fixed array of Faraday cups and ion counters, and including an adjustable ion beam dispersion device.

Micromass in the UK introduced the IsoProbe MC-ICP-MS where an off-axis hexapole collision cell is mounted in a jacket between the second interface cone and a beam focusing system [5]. The cell is flushed with a low pressure inert gas which reduces the ion energy to less than 1 eV. Also spectral interferences such as ArC⁺, ArN⁺, ArO⁺, ArCl⁺, and Ar₂⁺ dimers produced in the atmospheric plasma, which interfere with ⁵²Cr⁺, ⁵⁴Fe⁺, ⁵⁶Fe⁺, ⁷⁵As⁺, and ⁸⁰Se⁺, respectively, are removed by collision-induced cleavage of the Ar–X bonds, allowing measurement isotope ratios at masses below 80. The remainder of the instrument comprises a magnetic mass separator and a multiple collector detection system.

Nu Instruments in the UK introduced the Nu Plasma MC-ICP-MS. This machine, as with the Plasma 54, was developed by P.A. Freedman who maintained the same basic concepts, but introduced a different design for almost all the modules. Essentially it is a forward geometry (electrostatic sector followed by magnetic sector), double focusing mass spectrometer with a C-shape configuration compared to the Sshape of the P54. The ion beam profile conversion system is of different construction and the electrostatic energy filter and the magnetic separator were changed in shape and size. The profound advance in this design is the multiple collector detection system. The detection module comprises an array of 15 fixed detectors, 12 Faraday cups, and three electron multipliers, in front of which a zoom lens system deflects each separated ion beam into a chosen detector. Also, one of the multipliers is equipped with a filter for cutting off the tail from highly abundant isotopes. A later model from Nu Instruments, the Nu1700, is a large geometry, high resolution MC-ICP-MS [6] that allows one to overcome most of the interferences.

Finnigan MAT in Germany introduced the Neptune MC-ICP-MS, a double focusing C-shape instrument with a large magnet providing 16% mass dispersion, movable collector array, and high resolution capability. Flat-topped peaks are achievable at *R*>4,000 [7].

When discussing isotope ratio measurements utilizing plasma ionization, several further phenomena should be mentioned. Isotopic fractionation is of utmost importance. It is caused by repulsive forces in the intensive positive ion beam emerging from the plasma and supersonic ion expansion through the sample cone. Both effects yield radial repulsion of the lighter isotope from the beam center, i.e., increasing the heavy mass over light mass ratio. The fractionation effect is inversely mass dependent from several per mils in uranium to more than 10% in lithium. It is constant in time, since fresh sample solution is continuously aspirated into the ion source. This is in contrast to TIMS ionization, where a fixed sample is used, permanently changing in composition as the lighter isotope is preferentially vaporized. Fractionation may be corrected in one of three techniques: (1) internal and (2) external normalization, including double spike method; and (3) "standard-sample-standard bracketing"; consecutive measurements of the same ratio in a sample and standard. Further details will be given when describing the ratio measurements in the elements discussed in this review.

ICP mass spectrometry is subject to other interferences originating from various sources. Spectral interferences are products of interactions between the carrier gas and atmospheric gases or the solvent molecules. As mentioned above they obscure the lower mass range. Sodium ions in the sample solution in the case of copper analysis may interfere as ArNa⁺ at mass 63. Further cases are molecular interferences such as oxides, nitrides, and hydrides of trace elements in the solution and isobaric ion interferences. These cases can be removed by using expensive high resolution MS. Other ways to reduce interferences include using of desolvation nebulizer and chromatographic separation of the analyte from the matrix prior to introduction into the MS. This separation is also necessary to prevent the additional effects of mass fractionation connected with the matrix effect. In the case of the heavy isotope ratio measurements, this fractionation is corrected by internal or external normalization, but in the case of standard-samplestandard bracketing, generally used for light masses correction, the analyte must be carefully and precisely separated from the matrix.

As with the stable isotopes of the light elements, the isotopic composition of a sample is given in δ units (‰) relative to standard (I is isotope, x and y are mass numbers).

$$\delta (\%) = [(^{x}I/^{y}I)_{sample}/(^{x}I/^{y}I)_{standard} - 1]x1000$$
 (1)

Generally, the isotope variations are derived from bracketing the measured sample ratio with the mean ratios of a standard measured before (std1) and after the sample run (std2), and are presented as deviations in parts per



1,000 of the measured ratio from that of the standard (normalizing) ratio:

$$\delta(\%) = \{(^{x}IJ'^{y}I)_{samp}/[(^{x}IJ'^{y}I)_{std1} + (^{x}IJ'^{y}I)_{std2}]/2 - 1\}x1000$$
 (2)

Results and discussion

Lithium

Lithium isotopes are of significant importance in a number of fields, such as geochemistry [8-11], astrophysics [12-13], nuclear technology [14], and biomedicine [15]. MC-ICP-MS opened new frontiers in Li isotope measurements by providing high precision data (<0.3%, 2σ). Lithium isotopes fractionate during hydrothermal processes, and significant variations may be observed in 7Li/6Li ratios in water derived from marine sedimentary rocks and from hydrothermal altered igneous rocks, thereby providing valuable information regarding regional ground-water flow paths. Lithium isotopes are a powerful tracer of recycling processes in the Earth. This is particularly the case for understanding the geochemical evolution of the Earth's mantle, because (a) Li is a moderately incompatible constituent of minerals in peridotite, (b) Li isotope ratios show large variations in the terrestrial system, caused by low-temperature fractionation and mixing, (c) Li is a fluidmobile element. Therefore, combined with existing geochemical information, its isotopes could be powerful geochemical tracers, especially for fluid-related (metasomatic) mantle processes. In recent years, almost all lithium isotope studies dealing with geological and related systems have applied the MC-ICP-MS measurement technique.

Lithium isotope ratio measurements require careful separation of Li from the matrix in natural samples. For solid samples, digestion and ion exchange chromatography separation are used in general; liquid samples are processed by chromatographic separation [16–21]. Acid leaching [22, 23] and direct resin techniques [24] are also applied. The most rapid method of separation was published by Hall et al. [21] for TIMS and modified at the Geological Survey of Israel for MC-ICP-MS. Any traces of Na, K, Mg, Sr, and Rb were detected using this modified method, so the samples were sufficiently pure for ratio measurements by Nu Plasma MC-ICP-MS.

The values of the ratio in standard L-SVEC NBS (NIST, Li_2CO_3) are $^6\text{Li}/^7\text{Li} = 0.0832 \pm 0.0002$ [25], and in seawater $^6\text{Li}/^7\text{Li} = 0.08015 \pm 0.00006$ [26]. A typical analysis sequence consists of blank, standard, blank, sample 1, blank, standard, blank, sample 2, and so on. Lithium ratio measurements exhibit time-dependent drifts and

random shifts. Tomascak et al. [16] reported a typical $^7\text{Li}/^6\text{Li}$ ratio drift for the L-SVEC standard from 12.7 to 12.3 during an 8-h period. Nishio and Nakai [17] rejected data when two successive measurements of the bracketing standard ratio shifted by more than 2‰. These authors also reported a stability of $\delta^7\text{Li} = +15.08 \pm 0.82$ (2 σ) for an inhouse isotope standard measured over an 8-month period. It is good practice to carry out the sample and standard measurements under identical instrumental and solution conditions. The analyte concentrations in both solutions should be as close as possible and the impurity levels identical and as low as possible.

It should be noted that sample purity in TIMS analysis relative to MC-ICP-MS is of major importance, since the large isotopic fractionation in Li is highly sensitive to impurities in the loaded sample, especially when Na and K are interfering elements [21]. It was reported that a Na/Li ratio greater than approximately 5 may cause unstable instrumental fractionation [16]. Moriguti and Nakamura [27] developed a four-step chromatographic separation for Li purification, allowing precise TIMS Li ratio analyses.

Bouman et al. [28] studied a wide range of Li samples originating from islands in the Pacific, Atlantic, and Indian Oceans. Thirty six samples and three standard materials were analyzed. The precision of these measurement are 0.01–0.5(‰), 0.6–1.0(‰), and 1.2–1.9(‰) for 22, ten, and four samples, respectively. The data for standard materials are presented in Table 1, which also summarizes selected MC-ICP-MS Li isotope ratio measurements in geological samples.

Bryant et al. [29] studied Li isotope ratio measurements by MC-ICP-MS under "cold plasma" conditions. The results are characterized by fewer baseline interferences and improved reproducibility as compared with conventional hot plasma techniques. The 2σ precisions for 1,200-W, 800-W, and 680-W plasma energy are conservatively estimated as 1.1‰, 0.7‰, and 0.5‰, respectively. The effects of analyte, acid, and matrix concentrations were discussed.

Seitz et al. [31] determined the Li isotopic composition of coexisting olivine, clinopyroxene, and orthopyroxene from spinel- and garnet-bearing peridotite xenoliths. The degree of intramineral fractionation correlated negatively with equilibration temperature.

The lithium isotopic composition of saprolites developed on a granite and diabase dike from South Carolina was measured to document their behavior during continental weathering. A general trend of decreasing $\delta^7 \text{Li}$ with increasing weathering intensity was observed [32, 33]. A similar study was carried out by Kısakürek et al. [34]. The internal precision on $^7 \text{Li}/^6 \text{Li}$ measurements was usually less than 0.20‰, and the external precision of Nu Plasma MC-ICP-MS, was 0.8‰.



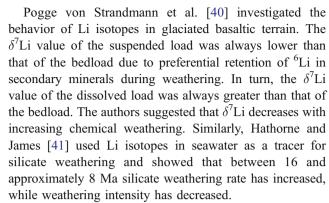
Table 1 Li isotopic composition in standards and selected natural samples relative to NIST NBS L-SVEC (‰)

Sample	δ^7 Li	$\pm 2\sigma$	Reference
JR-2 rock standard	3.84	0.18	[24]
Magmatic arc lavas (Kurile)			[18]
8322/3 Onekotan	4.2	<1.0	
K33 Keli-Mutu	5.1	<1.0	
VB30 granite	-1.4	1.0	[19]
MG20 granite	0.8	1.0	
Inorganic calcite CM019	-7.6	0.6	[20]
Coral Acropora	21.0	0.4	
Indian Ocean water	33.0	1.2	[21]
Atlantic Ocean water	32.1	1.2	
Foraminifera Orbulina universa	28.4	1.6	
Inorganically grown carbonates			[23]
Aragonite (salinity 10 psu)	-10.9	0.8	
Calcite (salinity 50 psu)	-1.9	0.8	
Seawater	29.7	0.4	[28]
BHVO-1 rock standard	5.0	1.5	
Seawater 680 W	30.7	0.4	[29]
Mediterranean Sea	30.59	0.26	[30]
Red Sea	30.49	0.12	
Dead Sea	28.78	0.11	
Yarkon spring	15.14	0.21	
SC -1 olivine	3.4	1.0	[31]
Ia/211 clinopyroxene	-2.4	1.0	
M 1 saprolite	-11.6	1	[32]
10 saprolite	0.2	1	
SH 65 Ocean Island basalt	7.0	<1	[35]
KRS9806 xenolith, Japan	-7.7	0.83	[36]
9708 xenolith, Australia	6.0	0.83	
Zagami meteorite	4.4	0.5	[38]
15495 lunar low-Ti mare basalt	5.6	0.2	
14-1 amphibolite	0.9	1	[39]
12-2 amphibolite	-14.2	1	

Ryan et al. [35] defined lithium isotope variations in mantle sources (volcanic rocks from the Antarctica oceanic islands), and Nishio et al. defined lithium isotope variations in mantle-derived xenoliths [36]. These isotopic measurements have provided much information on the mantle source region. Similarly, Elliott et al. [37] showed that Li isotopes promise to provide significant new constraints on the distribution of recycled material in the mantle and its implications for mantle convection.

Lithium isotope compositions and concentrations of lunar samples, including basalts, breccias, and glass, and martian meteorites were measured using Thermo Finnigan MC-ICP-MS [38].

Teng et al. [39] measured lithium isotopic compositions in the country-rock amphibolites and schists using Nu Plasma MC-ICP-MS. δ^7 Li decreased dramatically with contact distance (along a -10 m traverse from the pegmatite into amphibolite) from +7.6 to -19.9.



Nishio et al. [42] studied Li isotope ratios in North Atlantic and Indian Ocean waters and its relation to those of Sr and Nd. The Li isotope results support the recent proposal that significant amounts of recycled lower continental crust might produce the radiogenic isotope signatures of the Indian Ocean basalts. Rudnick and Ionov [43] examined Li isotopic disequilibrium in olivine and clinopyroxenes from far-east Russia. Jeffcoate et al. [44] studied Li isotope fractionation in peridotites and mafic melts. Their results highlight the potential of Li isotopes as a high resolution geospeedometer of the final phases of magmatic activity and cooling. Wunder et al. [45] studied Li isotope fractionation between Li-bearing staurolite, Li-mica, and aqueous fluids.

Magnesium

Magnesium has three naturally occurring isotopes at mass numbers 24, 25, and 26 with relative abundance of 78.99, 10.00, and 11.01%, respectively. Galy et al. [46] briefly summarized the various fields where natural variations in the isotopic composition of this element may arise: (1) stellar nucleosynthesis and incorporation of presolar grains into meteorites, (2) the decay of ²⁶Al to ²⁶Mg, (3) isotopic fractionation in volatilization/condensation reactions, (4) isotopic fractionation during low temperature fluid/rock interactions, and (5) kinetic and thermodynamic isotope effects in biological processes.

Galy et al. [46] performed high precision magnesium isotope ratio measurements using MC-ICP-MS for three groups of materials: commercial Mg materials including the NIST isotopic standard SRM 980, natural magnesite, and commercial chlorophyll in spinach. The observed ratio 26 Mg/ 24 Mg was 0.139828 ± 0.000037 (2σ), compared to the NIST value of 0.13932 ± 0.000 6 (2σ) [47]. The variations in the Mg materials reported in δ^{25} Mg and δ^{26} Mg units are given in Table 2. A desolvation nebulizer was used to minimize the introduction of H₂O, CO₂, O₂, and N₂, therefore reducing the presence in the plasma of molecular interferences such as C_2^+ , C_2H^+ , $C_2H_2^+$, CN^+ , and NaH $^+$. Other possible interferences are doubly charged ions such



Table 2 Mg isotopic composition in standards and selected natural samples relative to DSM-3 (‰)

	-26		a25		
Sample	$\delta^{26}{ m Mg}$	$\pm 2\sigma$	$\delta^{25}{ m Mg}$	$\pm 2\sigma$	Reference
Aldrich Mg solution	2.60	0.17	1.33	0.08	[46] ^a
Dead Sea Mg metal	3.96	0.15	2.03	0.08	
AG 177 magnesia	2.03	0.04	1.03	0.01	
OUM 10988 magnesite, Italy	1.22	0.04	0.60	0.03	
AG 27 chlorophill b, spinach	1.06	0.07	0.54	0.03	
North Atlantic Sea water	2.59	0.04	1.33	0.08	[51] ^a
Mixed foraminifera	-1.88	0.16	-0.99	0.10	
Dolomite	1.64	0.04	0.88	0.01	
Seawater					[52] ^a
EPR1 surface	1.95	0.14	0.98	0.06	
WP45N 5800 m	2.01	0.16	1.00	0.04	
Med-T1 surface	2.02	0.07	1.05	0.09	
Hydrothermal 2,650 m	-1.01	0.16	-0.51	0.06	
River water					
MB16	0.76	0.46	0.38	0.22	
MB6	0.09	0.22	0.04	0.11	
PH6	0.22	0.06	0.11	0.06	
PH5	-1.01	0.16	-0.51	0.14	
Ganges	-1.39	0.06	-0.7	0.09	[53]
Amazon	-1.03	0.07	-0.53	0.04	
Lena	-1.28	0.08	-0.66	0.02	
Seawater	-0.84	0.13	0.43	0.15	[54]
MT 66 solute	-1.74	0.07	-0.90	0.07	
Ett113 bulk silicate rock	-0.42	0.03	-0.21	0.02	
M 201 biotite	-0.07	0.09	-0.01	0.00	
MO33 100-110 soil	0.02	0.01	0.01	0.01	
Ace78 travertine	-4.01	0.11	-2.06	0.07	
Dead Sea water	-0.60	0.08	-0.33	0.10	[55]
Seawater	-0.74	0.05	-0.36	0.12	
Sataf spring	-2.50	0.10	-1.30	0.10	
Carbonaceous chondrites					[56]
144A, Al-Ti diopside	0.11	0.06	-0.09	0.12	
144A, Al-Ti diopside	-2.74	0.11	-1.74	0.11	
Olivines					[57]
DR9894 Australia	-1.43	0.2	-0.66	0.13	
ZS56-2 Siberia	-1.05	0.2	-0.54	0.13	

^a Relative to NIST isotopic standard SRM 980

as 48 Ca²⁺, 48 Ti²⁺, 50 Ti²⁺, 50 V²⁺, 50 Cr²⁺, and 52 Cr²⁺. These elements, if present, should be removed by purification.

Variations of the Mg isotope ratio in the metallic chips of the NIST SRM 980 magnesium isotopic standard were shown using five different MC-ICP-MS instruments of two types [48]. The chips were 1–50 mg in size. The differences in δ^{25} Mg and δ^{26} Mg of the SRM 980 were up to 4.2 and 8.19‰, respectively, while the long-term repeatability of the δ values was up to 0.09 and 0.16‰ respectively. Because of the heterogeneity of the NIST reference material, two homogeneous isotope standards, DSM-3 (Dead Sea magnesium) and Cambridge1 were prepared and characterized. The heterogeneity of Mg isotopes was also reported by Zhu et al. [49]. Carignan et al. [50] discussed the isotopic homogeneity of existing reference materials and suggested the acceptance of DMS-3 as a new Mg isotope reference standard material.

Chang et al. [51] developed a Mg separation technique for low-Mg biogenic carbonates with yields close to 100%. The technique was applied to the determination of Mg isotopes in three natural samples: seawater, foraminifera, and dolomite. De Villiers et al. [52] established the magnesium isotopic composition of seawater and evaluated its constancy as a function of depth and geographic location. The authors demonstrated that the magnesium isotopic composition of ancient oceans can be used to make important inferences about the relative contribution of different lithologies to the global continental weathering flux.

Tipper et al. [53, 54] analyzed river water, rock, travertine, and soil and demonstrated that both Ca and Mg isotope ratios are fractionated during weathering. The Mg isotope composition of the rivers is intermediate between limestone and silicate rock. Silicate soil has a δ^{26} Mg of -0.03%, heavier than that of silicate rock by 0.5%. This



fractionation in the soil creates a complementary ground-water reservoir of light Mg. Seasonal variations in Mg isotope ratios in the dissolved load are small, but define an array which can be modeled as a mixture between a fractionated groundwater reservoir and surface runoff.

Mg isotope fractionation during brine evolution in the Dead Sea is presently being studied using the MC-ICP-MS technique [55]. Samples from the solar system were used for ²⁶Al-²⁶Mg dating, by measuring the variations in the Mg ratios using laser ablation combined with MC-ICP-MS [56].

Pearson et al. [57] investigated Mg isotopic variations in the lithospheric mantle by analyzing olivine in mantle-derived peridotite xenoliths and megacrysts using a laser-ablation microprobe and MC-ICP-MS. δ^{26} Mg ranges from -3.01 to +1.03% and δ^{25} Mg from -1.59 to +0.51%, relative to the magnesium isotopic standard DSM-3, were found. The in situ measurement of Mg isotopes thus provides a powerful new method for investigating processes in the mantle.

Calcium

Calcium has six stable isotopes at mass numbers 40, 42, 43, 44, 46, and 48 with relative abundance of 96.941, 0.647, 0.135, 2.086, 0.004, and 0.187%, respectively. Halicz et al. [58] studied in detail the MC-ICP-MS isotope ratio measurements of calcium. The more important points are discussed here. Under normal instrumental operation conditions it is not possible to use the isotope ⁴⁰Ca because it is masked by the intense ⁴⁰Ar⁺ ion beam. Furthermore, the ion dispersion of Ca isotopes is too large to allow the 48Ca-42Ca mass range to be accommodated on the multicollector array; therefore only ⁴²Ca, ⁴³Ca, and ⁴⁴Ca are monitored. Arscattered interferences were monitored at half masses for elevated background correction. Corrections of doubly charged Sr were made by measuring doubly charged ⁸⁷Sr²⁺. A desolvation nebulizer was used to reduce molecular interferences such as $^{14}N_2^{16}O^+$, $^{12}C^{16}O_2^+$, and $^{40}ArH_2^+$. The results for the Ca ratios in the studied sample are given in δ units in Table 3 and were derived using the bracketing technique relative to the NIST SRM 915a Ca standard.

Wieser et al. [59] developed a high precision Ca isotope ratio measurement technique for a Finnigan Neptune magnetic sector ICP-MS. Delta values including δ^{44} Ca/ 43 Ca, δ^{44} Ca/ 42 Ca, and δ^{48} Ca/ 42 Ca were measured with an external reproducibility better than 0.2‰ in seawater and biogenic and non-biogenic marine carbonates. Fietzke et al. [60] developed a new technique for direct measurements of 44 Ca/ 40 Ca ratios on an MC-ICP-MS using "cool plasma". Reducing the plasma energy from the usually applied approximately 1,300 W to about 400 W significantly reduced the 40 Ar $^{+}$ isobaric effect, allowing simultaneous and precise measurements of the two Ca isotopes. Repeated measurements of the

Table 3 Ca isotopic composition in standards and selected natural samples relative to NIST SRM 915a (‰)

Sample	δ^{44} Ca	$\pm 2\sigma$	Reference
CaCO ₃ Merck	0.61	0.28	[58]
2-8-E3 speleothem	0.25	0.32	
Acropora coral	0.58	0.16	
Shell from marine organism			[59]
USGS EN-1	0.53 ^a	0.07	
CaCO ₃ JM 9912	-0.63	0.07	
CaCO ₃ JM 4064	-6.62	0.08	
Inorganic calcite			[61]
CM040	0.09	0.2	
CM039	-0.07	0.2	
Growth solution	0.31	0.2	
Foraminifera			[62]
OMEX-12b	0.21	0.10	
WIND-10b	0.28	0.11	
Mediterranean Sea water	0.98	0.14	
Seawater	1.09	0.09	[54]
MT 66 solute	0.54	0.06	
Ett113 bulk silicate rock	0.31	0.05	
MO33 0-10 soil	0.51	0.05	
MO33 100-110 soil	0.54	0.13	
Ace78 travertine	0.14	0.05	
Carbonate fluorapatite			[63]
OG-5	0.26	0.11	
D4/01	0.42	0.08	
S30/03	0.23	0.01	
32a/01	0.52	0.12	
32/01s	0.13	0.03	
D49/01	-0.23	0.06	

^a Relative to IAPSO seawater

⁴⁴Ca/⁴⁰Ca ratios in various Ca standard materials were in good agreement with data reported in the literature.

Marriott et al. [61] investigated temperature dependence of Ca isotopes in solution, inorganic calcite, and foraminifera and concluded that they are lighter than in the growth solution, and only weakly dependent on temperature. Sime et al. [62] also found negligible temperature dependence of calcium isotope fractionation in planktonic foraminifera.

River water, rock, travertine, and soil were studied by Tipper et al. [54] who demonstrated that Ca, as well as Mg isotope ratios, are fractionated during weathering. Fractionation of Ca during continental weathering is of importance to the global cycle of Ca. The riverine input of Ca to the oceans is controlled not only by the composition of the primary continental crust, but also by the size and composition of the fractionated reservoir on the continents. The impact on the oceanic cycle of Ca depends on the relative residence times of dissolved Ca in the ocean and the storage time of fractionated Ca.

Soudry et al. [63] explained fluctuations of Tethyan phosphogenesis through time, and whether or not they reflect long-term changes in ocean circulation or in



continental weathering. A δ^{44} Ca increase during the Late Cretaceous–Eocene also reflects a decrease in weathering Ca²⁺ fluxes together with increased biological removal of isotopically light Ca²⁺, fostered by increased continental flooding and concomitant carbonate (chalk) sedimentation on shelves. The overall concordant trends between the measured δ^{44} Ca, the eustatic sea level curve, and the sizes of the flooded continental area throughout the Early Cretaceous–Eocene, point to a linkage between the Ca isotopic composition of paleoseawater and long-term paleogeographic and oceanographic changes.

Steuber and Buhl [64] analyzed the calcium isotope composition in modern and ancient marine carbonates. No significant temperature dependence of Ca isotope fractionation was found in Cretaceous shells. δ^{44} Ca of Cretaceous seawater was 0.3–0.4‰ lower than that of the modern ocean.

Chu et al. [65] developed a procedure for the precise determination of Ca isotope ratios in natural and organic samples, such as bones, milk, and other biological materials. The data demonstrated that geological/environmental conditions do not cause large variability and it was suggested that diet is the major cause for variations in bones; so Ca isotope ratios may serve as a paleodiet tracer.

Skeletal carbonates from the Tethyan realm were analyzed by Farkaš et al. [66]. The observed late Mesozoic $\delta^{44} Ca_{sw}$ was simulated using a Ca isotope mass balance model, and the results indicated that the variation in $\delta^{44} Ca_{sw}$ can be explained by changes in oceanic input fluxes of Ca that were independent of the carbonate ion fluxes.

Sime et al. [67] interpreted Ca isotope behavior in marine biogenic carbonates. The 18 million year record of planktonic foraminifera in the Atlantic averages δ^{44} Ca = $+0.37 \pm 0.10$ and is a good match to Neogene Ca isotope record based on foraminifera, but is not similar to those in bulk carbonates. There are also publications on Ca using seawater as a standard for normalization in the bracketing method.

Copper

Copper isotope ratio measurements have been used to determine natural isotope variations in ore geology, geochronology, and archaeometry [68, 69]. Three different types of ICP-MS instrument, a quadrupole, a single collector magnetic sector, and a multicollector magnetic sector instrument, were compared by Diemer et al. [70]. Although precision of results significantly differed, excellent agreement was observed between results obtained using all the instruments. The results for the Cu-isotopic composition are given in Table 4.

MC-ICP-MS ratio determinations of copper were comprehensively studied by Zhu et al. [71]. A sample purification procedure was described, noting that possible isotope fractionation must be avoided. Potential interferences in 65 Cu/ 63 Cu ratio measurements are (23 Na 40 Ar)⁺ and

Table 4 Cu isotopic composition in standards and selected natural samples relative to SRM NIST 976 (%)

Sample	δ^{65} Cu	$\pm 2\sigma$	Reference
Native copper			[71] ^a
OUM15126 Michigan, USA	0.45	0.06	
OUM00061 Yekaterinburg, Russia	-0.33	0.06	
OUM15127 Cornwall, England	0.41	0.06	
Minerals			
OUM23585 malachite, England	-0.26	0.06	
OUM1616 azurite, USA	1.59	0.06	
OUM25139 chalcopyrite, England	0.07	0.06	
Acc. Ser. 25300 chalcopyrite, Canada	0.40	0.06	
G-4 chalcopyrite, sulfide deposits	-0.44	0.06	
Ultra-pure Cu standards			[75]
JMC Cu Axiom	0.619	0.058	
JMC Cu IsoProbe	0.641	0.019	
IMP Cu IsoProbe	0.20	0.10	
IMP Cu IsoProbe	0.207	0.049	
Copper sulfide precipitates			[78]
A-Cu- 0 Cu(I)S bulk	0.70	0.06	
A-Cu- 0 Cu(I)S precipitated	-2.52	0.06	
A-Cu-48 Cu(I)S bulk	0.62	0.06	
A-Cu-48 Cu(I)S precipitated	-2.32	0.06	
C-Cu-0 Cu(OH) ₂ bulk	-0.26	0.06	
C-Cu-0 Cu(OH) ₂ precipitated	-0.54	0.06	
Chalcopyrite from the Grasberg			[73] ^a
deposit region			
F1-001 Grasberg skarn	0.107	0.031	
XC05-001 Ertsberg diorite	0.633	0.035	
ES-005 Ertsberg skarn	0.193	0.054	
XC22001 pyrite shell	0.218	0.023	
XC25-002 bornite-2.69 Dalum	-0.269	0.031	
Alexandrinka VHMS sulfides			[76]
SW-1(a) chalcopyrite	0.184	< 0.07	
SW-1(b) quartz	0.318	< 0.07	
HV-1(a) sphalerite	0.330	< 0.07	
CA-1 pyrite	0.054	< 0.07	
CB-1(b) covellite	-0.300	< 0.07	
CB-2(a) silicate	-0.058	< 0.07	
Supergene copper sulfides			[81]
Tt-1, El Teniente bornite	0.37	0.16	
Tt-6, El Teniente chalcopyrite	-0.15	0.16	
El-1, El Salvador chalcopyrite	0.81	0.16	
, 15			

 $^{^{\}rm a}$ Original results were given in ${\cal E}$ units (parts per 10,000) and have been converted to δ units

(²³Na₂¹⁶O¹H)⁺ at mass 63 and (²⁵Mg⁴⁰Ar)⁺ at mass 65. It has been shown that for samples where Na/Cu and Mg/Cu ratios are below 10⁻⁴ and 10⁻³, respectively, and under instrumental working conditions applied in this study, the abundances of the polyatomic ions relative to Na⁺ and Mg⁺ were approximately 10⁻⁴, i.e., isobaric interferences were negligible.

Two Cu isotope measurement procedures were used: the standard-sample-standard bracketing technique where var-



iations are calculated relative to Cu isotope standard (SRM NIST 976) as in Eq. 2, and the "doping" technique [2] where the sample is doped with Zn at a concentration Cu/Zn ratio close to 1. Early results were given in " ε " units, but in the last papers " δ " is accepted. A constant value of the ⁶⁸Zn/⁶⁶Zn ratio was used as a normalization factor to correct the measured ⁶⁵Cu/⁶³Cu ratios. External precision (2 σ) better than 0.03‰ and 0.06‰ was achieved by applying the doping and bracketing techniques, respectively [71]. Borrok et al. [72] presented a new method for efficient separation of Cu, Fe, and Zn from the greater concentrations of matrix elements using a single anion-exchange column with hydrochloric acid media.

The possibility of laser ablation combined with a MC-ICP-MS for Cu isotope ratio determinations was presented by Graham et al. [73] About 160 solid samples were analyzed with a 2σ uncertainty of approximately 0.04‰. Jackson and Günter [74] examined the influence of various processes of laser ablation on fractionation of the Cu isotope ratio. The data suggest that the dominant source of isotopic fractionation at high laser fluence was the preferential volatilisation of 63 Cu during incomplete vaporization and ionization in the ICP of particles greater than approximately 0.5 μ m in diameter.

Mason et al. [5, 75] performed a detailed study on spectral interferences across the mass range ⁶³Cu to ⁷⁰Zn and the mass discrimination corrections using two different MC-ICP-MS instruments: the double focusing VG Axiom and the single focusing Micromass IsoProbe. It was observed that the ion types and their intensities depend on the different instrumental configuration. The importance of removing problematic matrix components prior to the Cu and Zn measurements was also emphasized. Based on their method Mason et al. [76] studied Zn and Cu isotopic variability in the Alexandrinka sulfide ore deposit from the Urals, Russia. A further study on mass discrimination correction shows the importance of matrix removal, particularly Fe and Ti, the dependence of mass discrimination on Cu/Zn ratio in the solution and that sample introduction system with a desolvating membrane causes variable behavior of the Cu standard, probably due to variations in Cu oxidation state in the solution [77].

Ehrlich et al. [78] studied copper isotope fractionation between aqueous Cu(II) and CuS, the latter being precipitated from CuSO₄ solution with Na₂S under anoxic conditions. Using Ni as a doping agent and the standard-sample-standard bracketing technique a 2σ error of 0.06‰ was achieved. The mean fractionation factor at 20 °C was derived: $\Delta^{65}\text{Cu}(\text{Cu}(\text{II})\text{aq}-\text{CuS})=3.06\pm0.14$. Additional experiments over the temperature range 2–40 °C showed an inverse dependence of the fractionation factor on temperature. Markl et al. [79] used copper isotopes as monitors of redox processes in hydrothermal mineralization. The authors concluded that

copper isotope analyses cannot be easily used as a reliable fingerprint for the source of copper in archaeology and geology because the variation caused by redox processes within a single deposit is usually much larger than between deposits. However, Asael et al. [80] showed that systematically large Cu isotope fractionation occurred during redox processes in sedimentary copper ore deposits. Cu isotope fractionation was also observed in bacterial oxidizing environments [81].

The roles of Cu and Zn isotopes in chondrites and iron meteorites were studied by Luck at al. [82, 83]. A typical error (external precision) for δ^{65} Cu±0.4–0.5‰ was reported. Moynier et al. [84] investigated isotopic composition of zinc, copper, and iron in lunar samples.

Recently isotopic ratio studies of Cu and Zn were performed in seawater [85]. The very low concentration of these elements and high TDS matrix demanded development of preconcentration and purification, followed by separation processes. In this work accurate data and their uncertainties are given only for Zn.

Conclusions

We have reviewed a group of more than 60 papers that were published in the period from 2000 up to present. We also quote results from a few unpublished works made at the GSI. We have chosen to focus on the isotope ratio determinations of only four elements, namely lithium, magnesium, calcium, and copper, where high precision ratio measurements were for various reasons impossible to achieve with the early MC-ICP-MS instruments. The second-generation machines have detection systems with sufficient dispersion to accommodate Li ions and the capability to be tuned to partial mass numbers. The high resolution capability allows one in some cases to resolve interferences. New types of desolvation nebulizers allow significant reduction of solvent and atmospheric interferences and the "cold plasma" technique reduces nebulizing gas ion intensities. Consequently, precision ($\pm 2\sigma$) for $\delta^7 \text{Li}$, δ^{25} , ²⁶Mg, δ^{44} Ca, and δ^{65} Cu down to the range of (0.1– 0.2)%, (0.01-0.1)%, (0.05-0.1)% and (0.06-0.15)%, respectively, can now be achieved.

Acknowledgments The authors wish to express their thanks to Prof. Alan Mathews for his assistance and helpful remarks. We also wish to thank the referees for scrupulously reading the paper and their useful corrections.

References

- 1. Walder AJ, Freedman PA (1992) J Anal At Spectrom 7:571
- Walder AJ, Freedman PA, Platzner TI (1993) J Anal At Spectrom 8:19



- 3. Walder AJ (1997) In: Platzner TI (ed) Modern isotope ratio mass spectrometry, Chap 4. John Wiley & Sons
- Walder AJ, Abell ID, Platzner I, Freedman PA (1993) Spectrochim Acta 48B:397
- Mason TFD, Weiss DJ, Horstwood M, Parish RR, Russell SS, Mullane E, Coles BJ (2004) J Anal At Spectrom 19:209
- Halliday AN, Freedman PA, Oberli F, Baur H, Hillins S, Levasseur S, Leya I, Poitrasson F, Quitte G, Teutsch N, Weichert U, Williams H, Williams J (2002) Geochim Cosmochim Acta 62A:303
- Schwieters J, Hamster M, Jung G, Pesch R, Rottmann L, Tuttas D (1999) Finnigan Mat Gmbh, Bremen, Germany, Part No. 19907200, 08/1999
- 8. Moriguti T. Nakamura E (1998) Earth Planet Sci Lett 163:167
- Chan LH, Edmond JM, Thompson G, Gillis K (1992) Earth Planet Sci Lett 108:151
- 10. Chan LH, Leeman WP, You CF (1999) Chem Geol 160:255
- 11. Tomascak PH, Ryan JG, Defant MJ (2000) Geology 28:507
- 12. Olive KA, Schramm DN (1992) Nature 360:439
- Knauth DC, Federman SR, Lambert DL, Crane P (2002) Nature 405:656
- 14. Lamberty A, de Bievre P (1986) CBNM-MS-G 45
- 15. Nishizawa K, Watanabe H (1986) J Nucl Sci Technol 23:843
- Tomascak PB, Carlson RW, Schirey SB (1999) Chem Geol 158:145
- 17. Nishio Y, Nakai S (2002) Anal Chim Acta 456:271
- Tomascak PB, Widom E, Barton LD, Goldstein SL, Ryan JG (2002) Earth Planet Sci Lett 196:227
- Teng F-Z, McDonough WF, Rudnick RL, Dalpe C, Tomascak PB, Chappell BW, Gao S (2004) Geochim Cosmochim Acta 68:4167
- Marriott CS, Henderson GM, Belshaw NS, Tudhope AW (2004)
 Earth Planet Sci Lett 222:615
- Hall JM, Chan L-H, McDonough WF, Turekian KK (2005) Marine Geol 217:255
- 22. Pistiner JS, Henderson GM (2003) Earth Planet Sci Lett 214:327
- Marriott CS, Henderson GM, Crompton R, Staubwasser M, Shaw S (2004) Chem Geol 212:5
- Magna T, Wiechert UH, Halliday AN (2004) Int J Mass Spectrom 239:67
- Flesh GD, Anderson AR Jr, Svec HJ (1973) Int J Mass Spectrom Ion Processes 12:265
- 26. James RH, Palmer MR (2000) Chem Geol 166:319
- 27. Moriguti T, Nakamura E (1998) Chem Geol 145:91
- 28. Bouman C, Elliott TE, Vroon PZ (2004) Chem Geol 212:59
- Bryant CJ, McCulloch MT, Bennet VC (2003) J Anal At Spectrom 18:734
- 30. Segal I, Platzner IT, Halicz L (2007) unpublished results
- Seitz HM, Brey GP, Lahaye Y, Durali S, Weyer S (2004) Chem Geol 212:163
- 32. Rudnick RL, Tomascak PB, Njo HB, Gardner LR (2004) Chem Geol 212:45
- Halama R, McDonough WF, Rudnick RL, Keller J, Klaudius J (2007) Earth Planet Sci Lett 254:77
- Kısakürek B, Widdowson M, James RH (2004) Chem Geol 212:27
- 35. Ryan JG, Kyle PR (2004) Chem Geol 212:125
- 36. Nishio Y, Nakai S, Yamamoto J, Sumino H, Matsumoto T, Prikhod'ko VS, Arai S (2004) Earth Planet Sci Lett 217:245
- 37. Elliott T, Jeffcoate A, Bouman C (2004) Earth Planet Sci Lett 220:231
- Seitz HM, Brey GP, Weyer S, Durali S, Ott U, Münker C, Mezger K (2006) Earth Planet Sci Lett 245:6
- 39. Teng FZ, McDonough WF, Rudnick RL, Walker RJ (2006) Earth Planet Sci Lett 243:701
- Pogge von Strandmann PAE, Burton KW, James RH, van Calsteren P, Gíslason SR, Mokadem F (2006) Earth Planet Sci Lett 251:134

- 41. Hathorne EC, James RH (2006) Earth Planet Sci Lett 246:393
- 42. Nishio Y, Nakai S, Ishii T, Sano Y (2007) Geochim Cosmochim Acta 71:74
- 43. Rudnick RL, Ionov DA (2007) Earth Planet Sci Lett 256:278
- Jeffcoate AB, Elliott T, Kasemann SA, Ionov D, Cooper K, Brooker R (2007) Geochim Cosmochim Acta 71:202
- 45. Wunder B, Meixner A, Romer RL, Feenstra A, Schettler G, Heinrich W (2007) Chem Geol 238:277
- Galy A, Belshaw NS, Halicz L, O'Nions RK (2001) Int J Mass Spectrom 208:89
- Catanzaro EJ, Murphy TJ, Garner EL, Shields WR (1966) J Res Natl Bur Stand 70A:453
- Galy A, Joffe O, Janney PE, Williams RW, Cloquet C, Alard O, Hallicz L, Wadhwa M, Hutcheon ID, Ramon E, Carignan J (2003) J Anal At Spectrom 18:1352
- 49. Zhu X, He X, Yang Ch (2005) Acta Geosci Sinica 26:12
- Carignan J, Cardinal D, Eisenhauer A, Galy A, Rehkamper M, Wombacher F, Vigier N (2004) Geostand Geoanal Res 28:139
- Chang VT-C, Makishima A, Belshaw NS, O'Nions RK (2003) J Anal At Spectrom 18:296
- 52. de Villiers S, Dickson JAD, Ellam RM (2005) Chem Geol 216:133
- Tipper ET, Galy A, Gaillardet J, Bickle MJ, Elderfield H, Carder EA (2006) Earth Planet Sci Lett 250:241
- 54. Tipper T, Galy A, Bickle MJ (2006) Earth Planet Sci Lett 247:267
- 55. Gavrieli Y, Yoffe O, Halicz L, Tepliakov N, Burg A (2007) Earth Planet Sci Lett (in press)
- Simon JI, Young ED, Russell SS, Tonui EK, Dyl KA, Manning CE (2005) Earth Planet Sci Lett 238:272
- Pearson NJ, Griffin WL, Alard O, O'Reilly SY (2006) Chem Geol 226:115
- Halicz L, Galy A, Belshaw NS, O'Nions RK (1999) J Anal At Spectrom 14:1835
- Wieser ME, Buhl D, Bouman C, Schwieters J (2004) J Anal At Spectrom 19:844
- Fietzke J, Eisenhauer A, Gussone N, Bock B, Liebetrau V, Nagler ThF, Spero HJ, Bijma J, Dullo C (2004) Chem Geol 206:11
- Marriott CS, Henderson GM, Belshaw NS, Tudhope AW (2004)
 Earth Planet Sci Lett 222:615
- Sime NG, De La Rocha CL, Galy A (2005) Earth Planet Sci Lett 232:51
- Soudry D, Glenn CR, Nathan Y, Segal I, VonderHaar D (2006)
 Earth Sci Rev 78:27
- 64. Steuber T, Buhl D (2006) Geochim Cosmochim Acta 70:5507
- 65. Chu NC, Henderson GM, Belshaw NS, Hedges REM (2006) Appl Geochem 21:1656
- Farkaš J, Buhl D, Blenkinsop J, Veizer J (2007) Earth Planet Sci Lett 253:96
- 67. Sime NG, De La Rocha CL, Tipper ET, Tripati A, Galy A, Bickle MJ (2007) Geochim Cosmochim Acta (in press)
- 68. Marechal CN, Telouk P, Albarede F (1999) Chem Geol 156:251
- Schoenberg R, Naegler TF, Kramers JD (2001) Int J Mass Spectrom 197:85
- 70. Diemer J, Quétel CR, Taylor PDP (2002) J Anal At Spectrom 17:1137
- Zhu XK, O'Nions RK, Guo Y, Belshaw NS, Rickard D (2002) Chem Geol 163:139
- Borrok DM, Wanty RB, Ridley WI, Wolf R, Lamothe PJ, Adams M (2007) Chem Geol 242:400
- Graham S, Pearson N, Jackson S, Griffin W, O'Reilly SY (2004) Chem Geol 207:147
- 74. Jackson SE, Günther D (2003) JAAS 18:205
- 75. Mason TFD, Weiss DJ, Horstwood M, Parish RR, Russell SS, Mullane E, Coles BJ (2004) J Anal At Spectrom 19:218
- Mason TFD, Weiss DJ, Chapman JB, Wilkinson J, Tessalinac SG, Spiro B, Horstwood MSA, Spratt J, Coles BJ (2005) Chem Geol 221:170
- 77. Archer C, Vance D (2004) J Anal At Spectrom 19:656

- Ehrlich S, Butler I, Halicz L, Rickard D, Oldroyd A, Matthews A (2004) Chem Geol 209:259
- Markl G, Lahaye Y, Schwinn G (2006) Geochim Cosmochim Acta 70:4215
- 80. Asael D, Matthews A, Bar-Matthews M, Halicz L (2007) Chem Geol (in press)
- 81. Mathur R, Ruiz J, Titley S, Liermann L, Buss H, Brantley S (2005) Geochim Cosmochim Acta 69:5233
- 82. Luck JM, Ben Othman D, Barrat JA, Albarède F (2003) Geochim Cosmochim Acta 143
- 83. Luck JM, Ben Othman D, Albarède F (2005) Geochim Cosmochim Acta 69:5351
- 84. Moynier F, Albarède F, Herzog GF (2006) Geochim Cosmochim Acta 70:6103
- 85. Bermin J, Vance D, Archer C, Statham PJ (2006) Chem Geol 226:280

